



PAPER • OPEN ACCESS

Influence of flow patterns on the performance of straight-through labyrinth seals. Numerical study and validation against experimental data

To cite this article: A Rocca *et al* 2021 *IOP Conf. Ser.: Earth Environ. Sci.* **774** 012032

View the [article online](#) for updates and enhancements.

| | |
|--|--|
|  <p>The Electrochemical Society Advancing solid state & electrochemical science & technology 2021 Virtual Education</p> <p>Fundamentals of Electrochemistry: Basic Theory and Kinetic Methods Instructed by: Dr. James Noël Sun, Sept 19 & Mon, Sept 20 at 12h–15h ET</p> <p>Register early and save!</p> |  |
|--|--|

Influence of flow patterns on the performance of straight-through labyrinth seals. Numerical study and validation against experimental data

A Rocca, S Troyer, A Casetta

Troyer SpA Via Karl von Etzel 2 - 39049 Vipiteno (BZ), IT

E-mail: andrea.rocca@troyer.it, stefan.troyer@troyer.it

Abstract. When numerically simulating the performance of a complete Francis turbine, it is common practice to omit the seals to save computing power. Volumetric and friction losses are usually taken into account using empirical values. There is abundant literature on the topic, but all analytic formulations rely on widely variable empirical coefficients. To overcome the uncertainty in determining volumetric losses, a detailed analysis of the sealing is necessary. Focusing on straight seals and configurations with cavities, in-house experimental data and numerical simulations have been used to show that few geometric parameters play a fundamental role in defining the flow patterns inside the clearance and even more so inside and between cavities. As is to be expected, the seals effectiveness is heavily influenced by these flow structures. It is also shown that certain methods of dealing with near-wall flow structures are better suited than others for the estimation of the discharge behaviour when compared to experimental results. Even though in the framework of the RANS equations CFD has proven to be a reliable tool for a wide range of geometries, further investigations are necessary on deep cavities. For aspect ratios above 0.75, the flow patterns inside the cavity change drastically, leading to bad convergence rates of the solver and, more important, to a considerable misalignment between numerical and experimental results. Lid-driven cavity flow is known to be a complex problem in 2D domain, and in this case, the flow becomes three-dimensional due to the tangential velocity induced by rotation. However, the reasons behind the problems in CFD analysis are not entirely clear. Given the observed variations of the flow structures inside sealings with different geometric parameters, it becomes clear why a simplified, generic formulation is very difficult to obtain, if not by adopting empirically defined coefficients which are needed to tune the analytical model.

1. Introduction

Seals have been used and studied by engineers for over a century. In this work we focus on incompressible fluids and straight (or see-through) seals with and without cavities on the stator. For simplicity, we will refer to the two configurations as "straight seals" and "seals with cavities".

There are many scientific works about seals but no universal behaviour has yet been found. The multitude of influencing factors has been taken into account by introducing empirical constants which vary in rather wide ranges. Early experimental works about this topic focused on understanding the flow through annular clearances with static and moving boundaries [1], [2], [3]. Trutnovsky's book [4] offers an excellent overview, reviewing eight different calculation methods for seals with cavities and incompressible fluids alone, as well as 25 experimental works and citing a bibliography of 368 publications. This underlines the complexity of the topic and during our work it was confirmed once more that, as Trutnovsky repeats many times, it is not possible to find a universal formulation.



Only more recently increasing computational power made it possible to numerically solve viscous turbulent flows for industrial applications. This allowed engineers to investigate these topics, even though they are not of primary academic interest any more. Today we have many different examples of CFD works which solve the Reynolds Averaged Navier-Stokes (RANS) equations, for two dimensional cases as [5], [6],[7], [8] and [9].

The two dimensional flow gives good results for some seal configurations. Le Roy, Guibault and Vu, [5], for example, predict the discharge coefficient with good approximation remaining below the experimental value. They use the commercial code CFX solving the equations up to the viscous sublayer, which is the same approach we used in the present work.

There are also examples of complete Francis turbine flow simulations which include the seals, e.g. in Schiffer et al. [10]. The simulation of the seals in the complete turbine adds a computational load which is comparable to the cost of simulating the same machine without the seal. The computational resources required for such simulations are not available for everyone, making them unaffordable for everyday use. This is also one of the reasons why we focused on the seal as an isolated component.

The objective of the work was to provide a simple engineering tool, which allows the design engineers to verify the leakage flow rate of the seals in Francis turbines in small and medium hydro applications. The strict timelines and small economic margins in the small hydro business do not allow for a CFD-based optimization of the seals for every project. However, as said, the wide range for the empirical coefficients proposed in literature results in a high uncertainty in the analytic calculation of the flow rate. This led us to set up a series of experimental tests. The CFD simulations served to reach a better understanding of the flow inside the seal, while the experiments allowed us to validate the CFD simulations. The experience made over the course of the project proved how important this was. Finally, the combination of CFD and experiment allowed us to find a semi-analytic formulation for easy and yet satisfactory estimation of the leakage flow rate.

The paper is organised as follows. Section 2 gives the formulation of the problem, explaining the geometrical setup of the sealings and then passing on to the numerical formulation of the problem. In section 3 the results obtained from the numerical simulations are validated against experimental data, while section 4 introduces the semi-analytical model derived from the works of Yamada [3], Chebysheva [11] and Kovalev [12]. Section 5 discusses the dissipation mechanism in seals with cavities based on the energy transfer from the main flow towards turbulent kinetic energy as described by Pope [13] and Davidson [14]. A way to optimize the design based on the physics behind the dissipation mechanism is also proposed in section 5, while the key geometrical parameter determining the flow through seals with cavities, the cavity aspect ratio ξ , is analysed more thoroughly in section 6.

2. Formulation of the problem

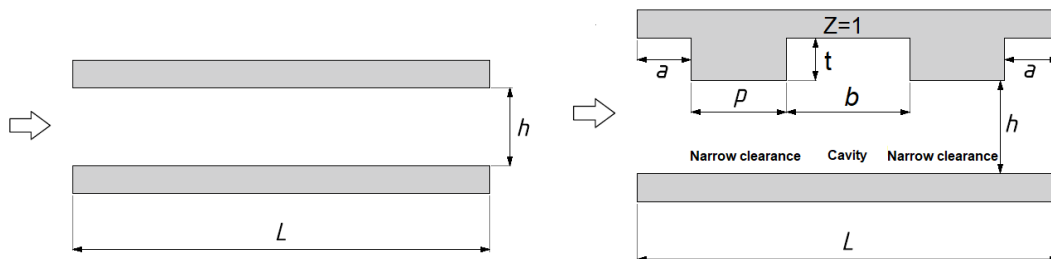
2.1. Geometry description

A brief description of the geometry will follow in the next two subsections. Table 1 lists the nomenclature and the symbols used in the present work.

2.1.1. Straight seals without cavities The geometry of a straight seal is determined by three parameters. They are the radius of the rotor r_1 , the clearance height h and the seal's length L . A longitudinal section is sketched in figure 1.

2.1.2. Seals with cavities on the stator Figure 2 shows a schematic longitudinal section of the seal with cavities. To completely describe this geometry four additional parameters are needed. We considered only configurations with identical cavities. The number of cavities inside a single seal passage is Z . The axial distance between two adjacent cavities is p . The cavity height is indicated using the symbol t while the cavity axial length is b . These two parameters define the cavity aspect ratio called ξ , while the lengths of the inlet and outlet clearances are indicated by a .

| Quantity | Symbol | Units |
|--|------------|---------|
| Radius of the rotor | r_1 | mm |
| Radius of the stator | r_2 | mm |
| narrow clearance height | h | mm |
| cavity height | t | mm |
| cavity axial length | b | mm |
| axial distance between two adjacent cavities | p | mm |
| number of cavities | Z | - |
| cavity aspect ratio | $\xi=t/b$ | - |
| seal length | L | mm |
| rotational speed | n | rev/min |
| pressure at the inlet | P_1 | bar |
| pressure at the outlet | P_2 | bar |
| mass flow rate | Q | m^3/s |
| head loss across the seal | H | m |
| pressure drop across the seal | Δp | Pa |

Table 1. List of symbols**Figure 1.** Straight seal without cavities**Figure 2.** Seal with one cavity on the stator

2.2. Numerical Formulation

Steady-state RANS simulations were carried out using the commercial software ANSYS CFX. To simplify the problem and to find a reasonable compromise between accuracy and computational cost, we made the hypothesis that a steady solution exists and that the flow is periodic in the circumferential direction. This hypothesis allows us to reduce the computational domain in circumferential direction as shown in figures 3 and 5, verifying a posteriori that the circumferential extension of the domain was not influencing the results. Instead of including the chambers upstream and downstream of the seal, a loss coefficient at the inlet of the computational domain was introduced (see also eq. 2). The approach chosen is that of solving the RANS equations, without using any shear-stress model for the wall adjacent flow. Reynolds stresses are modelled under the Boussinesq eddy-viscosity hypothesis and closure is achieved by Menter's Shear Stress Transport model $k - \omega$ SST [15].

All the grids used are composed exclusively by hexahedra. The wall spacing is calculated to guarantee a $y^+ \approx 1$ everywhere at the rotor and stator surfaces. Velocity and wall-distance, scaled with wall length scales, match the statistical behaviour of the law-of the wall, as shown in figure 4.

Using Yamada's definition [3], the axial Reynolds number is calculated as $Re = \frac{h v_a}{\nu}$, where v_a is the axial velocity and h is the clearance height [12], [3].

For this class of problems, under these conditions, the axial Reynolds number is of the order of 10^4 .

Therefore the flow through the seal is turbulent and according to [16] we do not expect the formation of Taylor vortices. We will refer to SST model although also other models were tested as, for example, realizable $k-\epsilon$ [17] and Reynolds stress equation model [18].

The boundary conditions used are:

- inlet: "opening" with the specification of the total pressure
- outlet: "area averaged pressure"
- rotor: "rotating wall"
- stator: "stationary wall"
- periodicity boundary condition at the remaining two patches

Advective terms in the momentum equation are discretized using second order upwind, while in k and ω equations, divergence terms are discretized using a first order upwind. Pressure-velocity and $k - \omega$ are fully coupled.

The system reference frame has its origin at the inlet on the rotor, and passes through the symmetry plane of the seal. The z -axis is aligned with the streamwise direction while on the symmetry plane the y -axis points to the wall normal direction. We will also frequently refer to "circumferential" and "radial" directions.

2.3. Straight seal

The computational domain and the system reference frame are shown in figure 3. By means of the periodicity we were able to reduce the computational domain to only 5° in circumferential direction. Periodicity hypothesis holds well for straight seals.

Figure 3 shows the surface mesh on the stator. As already mentioned the mesh is thought to resolve the boundary layer up to the viscous sublayer. By this we can get a superior spatial resolution, clustering high density of cells everywhere in the computational volume, and more precise wall shear stress computation on rotor and stator. Using the wall functions, especially together with roughness models and h being very small, results in a low number of grid points in radial direction.

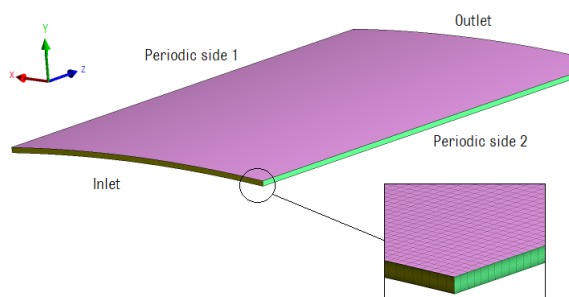


Figure 3. Straight seal's computational domain and grid.

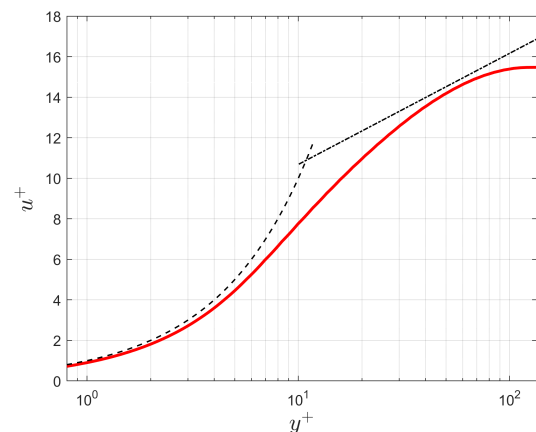


Figure 4. The law of the wall over the clearance height at $L/2$ from the inlet. Computation (—); $u^+ = y^+$ (- - -). The log law (- · -).

2.4. Seals with cavities on the stator

The computational domain and the system reference frame are shown in figure 5. We investigated several different configurations, varying the geometrical parameters and the pressure drop. The cavity aspect ratio was found to be a key parameter. We noticed that when increased, it strongly influences the flow behaviour and consequently the discharge rate.

Periodicity hypothesis hold well also for seals with cavities and aspect ratios $\xi \leq 0.4$. When $\xi \geq 0.5$ we observed a dependence of the flow variables on circumferential coordinates and the periodicity assumption could be physically incorrect.

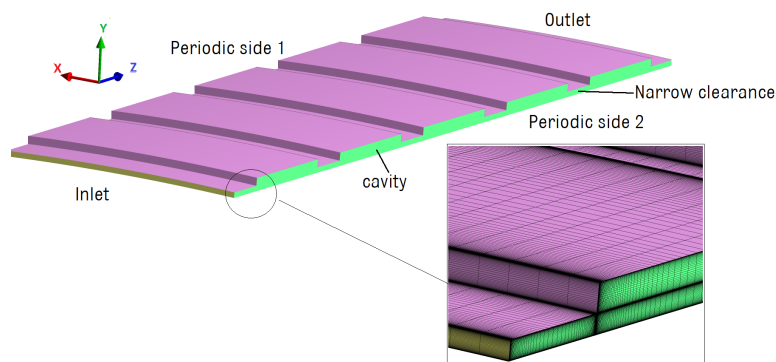


Figure 5. Seal with cavities on the stator. Computational domain and surface mesh on the stator.

We will refer to *narrow clearance* when considering the volume characterized by the height h and to *cavity* when speaking of the volume characterized by the height $h+t$ (see figure 5).

3. Validation of numerical simulation against experimental data

The validation of the numerical simulations against experimental data defines the range of applicability of our numerical setup and semi-analytic model. CFD carried out during this research project excellently works in a wide range of flow conditions. For seals with cavities, whose aspect ratio exceeds $\xi > 0.5$, we experienced difficulties in finding reasonable solutions in agreement with experimental data. For these configurations, numerical simulations failed to converge and did not match experimental data at all. Therefore, in the following sections only the results for straight seals and for seals with cavity aspect ratios $\xi < 0.5$ are analysed.

For the sake of conciseness, we will compare only selected configurations. The results for the other configurations we analysed are similar to those we selected.

Every mesh used is the result of a mesh refinement study. As example of grid convergence for a straight seal, increasing the cell count uniformly of 80% leads to a mass flow rate variation of 0.5% while, for a seal with cavities, an increasing of 45% of the cells count lead to a mass flow rate variation of 0.7%.

3.1. Experimental setup

The in-house experimental data were recorded using a test rig based on the one described in [5]. All tested sealings had a length of $L=40$ mm with an outer diameter of the rotating rings of 300 ± 0.5 mm. The nominal clearance height of the analysed configurations varied between $h=0.25$ mm and $h=0.60$ mm both for straight seals as well as for seals with cavities. The number of the evenly spaced cavities was either $Z=4$ or $Z=5$, depending on the cavity length b .

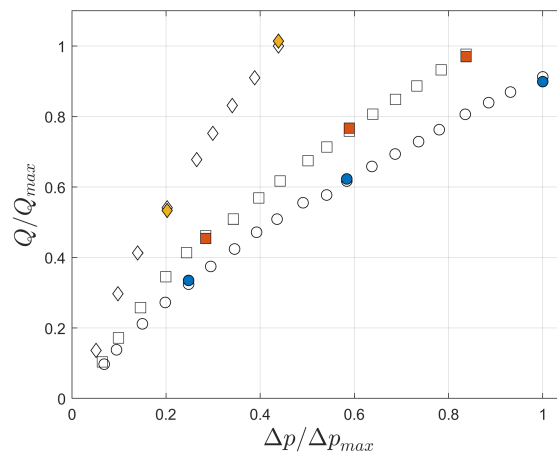


Figure 6. Straight seal: validation of numerical simulation against experimental data with constant rotational velocity.

$h/h_{min} = 1$: experimental data (\circ), numerical simulation (\bullet)

$h/h_{min} = 1.15$: experimental data (\square), numerical simulation (\blacksquare)

$h/h_{min} = 1.55$: experimental data (\diamond), numerical simulation (\blacklozenge)

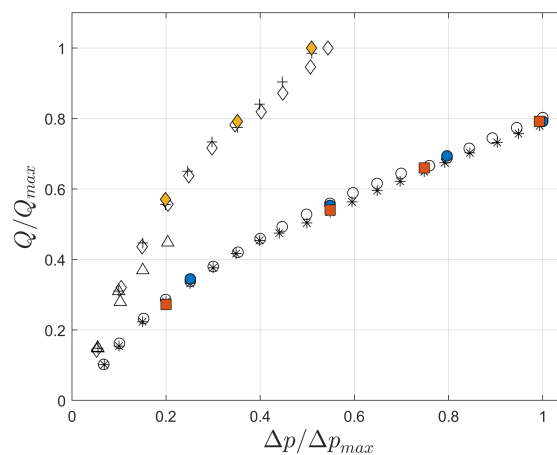


Figure 7. Seal with cavities: validation of numerical simulation against experimental data with constant rotational velocity.

$h/h_{min} = 1, \xi = 0.2$: experimental data (\circ), numerical simulation (\bullet)

$h/h_{min} = 1, \xi = 0.4$: experimental data ($*$), numerical simulation (\blacksquare)

$h/h_{min} = 1.15, \xi = 0.4$: experimental data (\diamond), numerical simulation (\blacklozenge)

$h/h_{min} = 1.15, \xi = 0.8$: experimental data ($+$)

$h/h_{min} = 2.25, \xi = 1.2$: experimental data (\triangle)

3.2. Simulation of straight seals

The flow through straight seals, with the wall surfaces considered hydraulically smooth, is simulated using the numerical setup presented previously in subsection 2.3. As an example, to simulate a straight seal with $h/(2r_1) = 9.02 \cdot 10^{-4}$ and $L/(2r_1) = 0.136$, the mesh described in table 2 was used.

For this case $Re_\theta = 13\,274$ and $Re_a = 7\,000$. The difference between experimental flow rate and numerical

| | Streamwise | Wall-normal | Circumferential | Total |
|-------------------|------------------|------------------|-----------------|---------|
| N. cells | 100 | 60 | 100 | 600 000 |
| distribution | single direction | double direction | uniform | - |
| transition factor | - | 1.105 | 1.015 | - |

Table 2. Grid characteristics in the three directions

simulation results was below 5% for all configurations.

3.3. Simulations of seals with cavities on the stator

For this type of seals the cavity aspect ratio ξ plays a fundamental role in determining the three dimensional vortex structures inside the cavity. This means that for different values of ξ , the numerical schemes must be adapted to correctly replicate these vortex structures. Explaining the ad-hoc treatment of the different cases in more detail would go well beyond the scope of this paper. The circumferential extension of the seal was further reduced, taking care to verify a-posteriori the validity of the periodic boundary condition. Thus, the mesh cell count was reduced to 1.44 M hexa-type cells keeping the same resolution in the case of $\xi = 0.4$, which is an intermediate case. When $\xi \leq 0.25$ the seal behaves as a straight seal with a finite number of obstacles causing local head loss. In the particular case of a seal with $Z=5$ cavities and $\xi = 0.2$, we found a very good agreement between numerical simulations and experimental data.

4. A semi-analytic model for discharge prediction

This model is based on the works of Yamada [3], Chebisheva [11] and Kovalev [12], where the discharge is calculated from Torricelli's law modified by a discharge factor μ . In particular we propose an improved formulation for μ that takes into account the shape of the cavities through the aspect ratio ξ .

$$Q = \mu A \sqrt{2gH} \quad (1)$$

$$\mu = \frac{C_1}{\sqrt{\frac{\lambda L}{2h} + \zeta_{in/out} + C_2 Z + \frac{1}{\xi}}} \quad (2)$$

where:

- A - Cross sectional area of the seal
- λ - friction loss factor (see eq. 3)
- C_1 - empirical constant
- C_2 - local losses at every cavity according to Kovalev [12]
- ξ - cavity aspect ratio
- $\zeta_{in/out} = 1.5$ - local losses at inlet (estimated as constant $0.5 v^2/2g$) and at outlet (complete dissipation, thus $1.0 v^2/2g$)

The empirical constant C_1 is needed to better replicate the experimental results, as the fit was found not to be satisfactory without this factor. The value of $C_2 = 1.1$ as given by Kovalev was confirmed by CFD simulations.

λ is calculated using the following empirical relation proposed by Yamada [3]:

$$\lambda = 0.27 Re_a^{-\frac{1}{4}} \left[1 + \left(\frac{7 Re_\theta}{16 Re_a} \right)^2 \right]^{\frac{3}{8}} \quad (3)$$

where the axial and circumferential Reynolds numbers are given according to Yamada's definition:

$$Re_a = \frac{h v_a}{\nu} = \frac{h Q}{2\pi r_1 h \nu} = \frac{Q}{2\pi r_1 \nu}$$

$$Re_\theta = \frac{2h v_\theta}{\nu} = \frac{2\pi r_2 n h}{60\nu}$$

Note that in most works, $2h$ is used as the characteristic dimension.

We tried different formulations for μ , including Chebysheva's approach which uses a variable resistance factor for the different shapes of cavities, multiplied by the number of cavities. Interestingly, the best fit was achieved with a formulation that does not entirely satisfy the physical instinct, as Chebysheva's formula does. In fact, the term for the aspect ratio is not multiplied by the number of cavities, because otherwise the influence of ξ would be overestimated.

The distance between the cavities p is neglected in our case, because, within certain limits and for reasons which will be explained in section 5, it should not be too big.

Straight seals can be considered as a particular case of equation number 2 where $Z=0$ and $1/\xi=0$.

Figure 8 shows the behaviour of the semi-analytic model against the experimental data (same experimental data as in figure 7). Except for few spurious points at dimensionless pressure values below 0.15, the model predicts the discharge with good accuracy. Figure 9 shows that the influence of rotational speed on the discharge is more pronounced for straight seals, which is a confirmation of most of the predictions found in the literature.

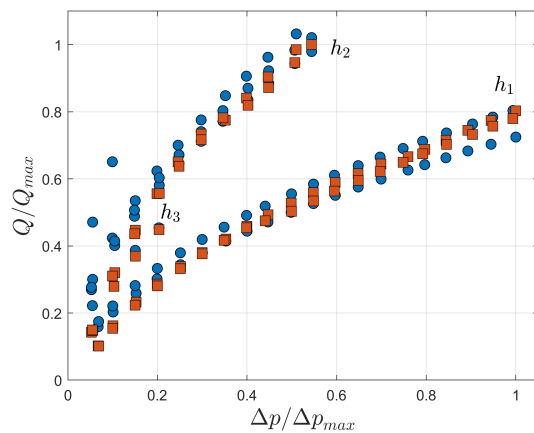


Figure 8. Seal with cavities, discharge rate Vs pressure drop, for constant rotating speed n and for three distinct seal heights h . Experimental data (■); semi-analytic model (●).

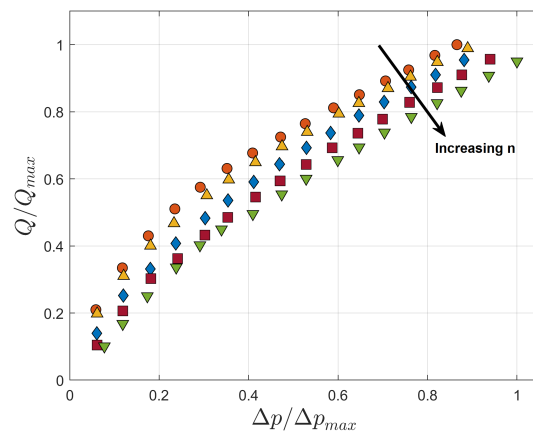


Figure 9. Straight seal, experimental data of the discharge rate Vs pressure drop for increasing rotating speed n and constant h . $n/n_{max} = 0.18$ (●); $n/n_{max} = 0.36$ (▲); $n/n_{max} = 0.53$ (◆); $n/n_{max} = 0.71$ (■); $n/n_{max} = 1$ (▼).

5. The dissipation mechanism

The efficiency of a seal is related to its ability to dissipate the fluid energy. In any three dimensional turbulent flow, statistically, the energy is subtracted from the mean field towards the fluctuations and goes from the large scales to small scales, where dissipation occurs [13], [14]. Following this simple reasoning, to investigate the seal performance we could follow the evolution of turbulent kinetic energy k . We prefer to focus our attention on k and in particular to its production term \mathcal{P} , since k is a measurable quantity.

In the framework of RANS and $k-\omega$ SST model, the model equation for the turbulent kinetic energy [13] defines the production term as a function of eddy viscosity and mean rate of strain:

$$\mathcal{P} = 2\nu_t \bar{S}_{ij} \bar{S}_{ij} \quad (4)$$

where \bar{S}_{ij} is the mean rate-of-strain tensor and ν_t is the eddy viscosity.

In a straight seal this equation can be approximated with only the transverse mean axial velocity gradient term, $\frac{\partial v_a}{\partial x_n}$ (with x_n the wall normal coordinate), while in a seal with cavities, the geometric discontinuities are responsible for the activation of the other terms involving derivatives of equation 4.

So our aim will be to design the seal in order to increment this phenomenon of energy transfer, monitoring the average value of k inside the control volume. Figure 10 shows colour map of k for a seal with cavities where the turbulent kinetic energy decreases through the narrow clearance.

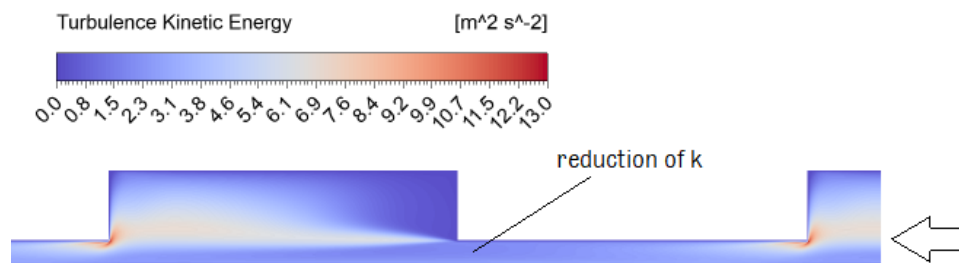


Figure 10. TKE contour plot in the narrow clearance

Reducing the distance between two adjacent cavities p by 50%, and maintaining the seal's length constant by extending the length of the inlet and outlet sections (see section 2.1), we calculated a reduction of 3.7% of mass flow rate. This suggests that long passages between two cavities are not efficient. The analysis of the contributions of the single terms to the discharge factor μ in eq. 2 suggested that an even better configuration could be obtained for this given seal length by adding an extra cavity, shortening p by 50% and also reducing the inlet and outlet clearance length a . In this case, from numerical simulation we computed a mass flow rate reduction of 6.3%, adding evidence to the hypothesis that the number of cavities is the leading term in the discharge factor equation.

6. The cavity aspect ratio

Figure 7 shows that increasing the cavity aspect ratio above a certain level may reduce the mass flow rate. Despite doubling the seal height h and with it the cross sectional area, when ξ passes from 0.8 (+ markers) to 1.2 (\triangle markers), the mass flow rate decreases significantly. This suggests that a change in the flow pattern inside the cavities has occurred and this leads to a different behaviour of the seal.

For this configuration, the experimental data are not supported by numerical simulations because of convergence issues (see figure 11(a)) and low accuracy in mass flow rate determination. Moreover, the experimental data collected in this range are limited. Shortly, we tested different numerical schemes, unsteadiness using URANS and alternative turbulence models to the $k-\omega$ SST. The periodicity assumption was verified using 360° geometries, where no significant improvements were registered.

According to the literature, we also have decided to adopt an even simpler two-dimensional numerical model of the seal which yielded the qualitative mass flow rate shown in figure 11(b).

This 2D-model does not take into account the rotation of the rotor but supports our physical arguments by predicting - qualitatively - the behaviour of the mass flow rate against the cavity aspect ratio for $\xi > 0.75$. However, for $\xi \leq 0.75$ it is not in agreement with the behaviour suggested by experimental data. In particular, for constant h and ξ increasing from 0.4 to 0.8, figure 7 shows a slight reduction of the

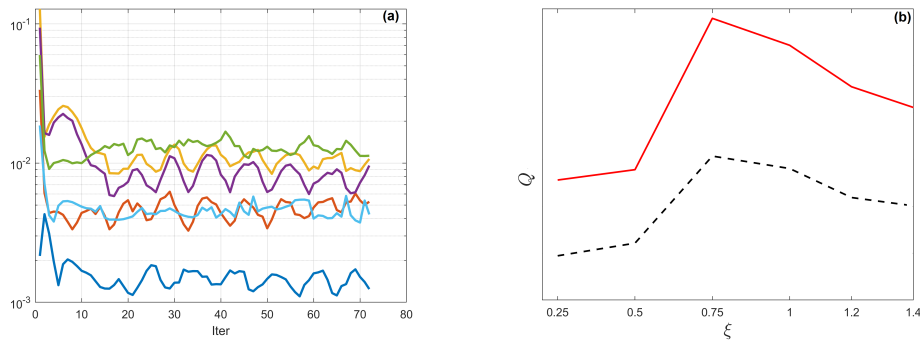


Figure 11. (a) Seal with cavities, $\xi = 1.2$ - Maximum residuals: p (—), u (—), v (—), w (—), k (—), ω (—). (b) Qualitative mass flow rate Q versus cavity aspect ratio (ξ) in 2D seal at $Re_a = 12730$. h_1 (---), h_2 (—). $h_1 < h_2$.

discharge, as suggested passing from * to \diamond symbols, while the sharp increase of the flow rate in figure 7 clearly contradicts this empirical evidence.

Further investigations are needed both on the numerical and experimental side. These changes in the flow patterns that determine different physics inside the seal constitute a big challenge when trying to analytically describe the discharge of a seal with cavities.

7. Conclusions

Straight seals and seals with cavities has been thoroughly analysed. We have found that the behaviour of seals with cavities is strongly influenced by the internal flow patterns that change with the cavity's aspect ratio.

Straight seals and seals with cavities with small ξ display a similar fluid dynamic behaviour to the point that the discharge coefficient μ converges to the same value for the seal with cavities and $\xi = 0.2$ and the straight seal at high rotational speed. However, at lower rotational speeds the performance of the seal with cavities is slightly superior.

For higher aspect ratios the discharge is drastically reduced. The amount of available experimental data is relatively small and the failing of 3D numerical simulations makes further investigations necessary. Our idea is that an eddy-viscosity assumption to model the Reynolds stress tensors it is not appropriate because the high three dimensionality of the flow. The periodicity assumption should also be investigated more in detail. Unfortunately, to simulate a complete seal using an higher order model for closure, the available computational power was not sufficient. The bi-dimensional numerical model is not affected by these issues but was found to be not well-aligned with experimental data.

Apart from the sealing clearance h , the single most important optimization parameter for seals with cavities appears to be a relatively high level of turbulent kinetic energy throughout the sealing. The energy transfer rate towards k is determined by various geometrical parameters such as the aspect ratio ξ , the distance between cavities p and the cavity length b . However, each of these parameters does not exercise it's influence independently, but there are strong links between them as the flow features introduced by the geometric discontinuities vary with the relations between the single parameters as well as with the axial and tangential Reynolds numbers.

By means of the comparison mentioned in section 5, it has been found that excessively long distances between cavities result in a higher discharge coefficient μ , because k is reduced and less energy is dissipated. This is perfectly in line with our statement that high levels of turbulent kinetic energy throughout the seals result in a lower discharge coefficient.

As an engineering design tool a semi-analytic model was developed. We added an extra term in the formulation of μ which takes into account the cavity's shape. Interestingly, the best fit was achieved with

a model not catering to the physical instinct. The empirical constant C_1 of equation 2 tunes the model to get a better agreement with the experimental data. We have found three different values for C_1 , one for straight seals, another for seals with cavities and small ξ and a third one for seals with cavities and high ξ . This allows us to maintain a handy analytic model at the cost to discern different flow categories.

The need to identify distinct flow categories derives from the fact that certain flow patterns develop depending on a combination of the geometric parameters of the seal as well as axial and tangential Reynolds numbers.

Therefore, it is clear why the simplified, semi-analytic model based on seemingly independent geometric parameters and tuned to fit experimental data can not be universally transferred to other configurations. This might also be the case for higher pressure differences, as the flow patterns determining the discharge coefficient may change with higher axial flow velocities.

To use the semi-analytic model in real applications it was necessary to improve its formulation to predict the discharge of a system of two or more seals, which is what typically is found in practical applications.

References

- [1] Cornish R J 1932 Flow of water through fine clearances with relative motion of the boundaries *A.M.I.Mech.E.*
- [2] Vermes G 1960 A fluid mechanics approach to the labyrinth seal leakage problem *ASME pub*
- [3] Yamada Y 1960 Resistance of a flow through an annulus with inner rotating cylinder *bulletin JSME*
- [4] Trutnovsky K 1973 *Berührungsfreie Dichtungen - Grundlagen und Anwendungen der Strömung durch Spalte und Labyrinth* 3rd ed (Dusseldorf: VDI-Verlag GmbH) ISBN 3184002802
- [5] LeRoy V, Guibault F and Vu T C 2009 Validation of a cfd model for hydraulic seals *Int. J. Fl. Mach. Sys.* **2**
- [6] Kim T S and Cha K S 2009 Comparative analysis of the influence of labyrinth seal configuration on leakage behavior *J. Mech. Sci. and Tech.* **23** 2830–2838
- [7] Schramm V, Denecke J, Kim S and Wittig S 2004 Shape optimization of a labyrinth seal applying the simulated annealing method *I. J. Rot. Mach.* **10** (5) 365–71
- [8] Zhao W, Nielsen T K and Billdal J T 2010 Effects of cavity on leakage loss in straight-through labyrinth seals *IOP Conf. Series: Earth and Envir. Sci.* **12**
- [9] Rhode D L and Nail G H 1992 Computation of cavity-by-cavity flow development in generic labyrinth seals *J. of Tribology* **114** (47)
- [10] Schiffer J, Benigni H, Jaberg H, Schneidhofer T and Ehrenguber M 2015 Numerical simulation of the flow in a francis turbine including the runner seals on crown and band side *Proceedings of HYDRO 2015 Conference.*
- [11] Chebysheva K V 1936 Study of a model of a labyrinth seal *Tekhn. Zanetki Tsentr. Aerogidrodinam. Inst.* **75**
- [12] Kovalev N N 1961 *Hydroturbines - design and construction* (GNTI)
- [13] Pope S 2001 *Turbulent flows* (Cambridge Press)
- [14] Davidson P 2015 *Turbulence: An Introduction for Scientists and Engineers* (Oxford University Press)
- [15] Menter F R 1994 Two-equation eddy-viscosity turbulence models for engineering applications *AIAA J.* **32** 1598–1605
- [16] Kaye J and Elgar E C 1958 Model of adiabatic and diabatic fluid flow in annulus with an inner rotating cylinder *Transactions of ASME* **80** (1) 753–65
- [17] Shih T H, Liou W W, Shabbir A, Yang Z and Zhu J 1995 A new $k - \epsilon$ eddy viscosity model for high reynolds number turbulent flows *Comp. Fluids.* **24** (3) 227–38
- [18] Wilcox D C 1993 *Turbulence modelling for CFD* (DCW Industries, La Cañada)